Journal of The Electrochemical Society, **149** (8) C406-C412 (2002)
0013-4651/2002/149(8)/C406/7/$7.00 © The Electrochemical Society, Inc.

Monte Carlo Simulation of the Electrodeposition of Copper

II. Acid Sulfate Solution with Blocking Additive

Timothy J. Pricer,[a,*] Mark J. Kushner,[b] and Richard C. Alkire,[c,,z]**

[a]*IBM Burlington Plant, Essex Junction, Vermont 05452, USA*
[c]*Department of Chemical Engineering and Frederick Seitz Materials Research Laboratory, and* [b]*Department of Electrical and Computer Engineering, University of Illinois, Urbana, Illinois 61801, USA*

Simulation of copper electrodeposition in the presence of a hypothetical blocking additive was carried out by a linked continuum/noncontinuum numerical code for various geometric configurations in the shape of a rectangular trench. The mechanism of copper electrodeposition described in Part I of this series was extended to include a single additive species. The hypothetical additive had the property that it blocks deposition but is consumed at the surface, and that its arrival at the electrode surface is transport-limited so that leveling occurs. With use of numerical simulations carried out with a linked Monte Carlo-finite difference code described in Part I, the effect on trench in-fill of additive concentration, adsorption rate, consumption (breakdown) rate, and trench aspect ratio was investigated.
 [DOI: 10.1149/1.1488649]

Manuscript submitted February 1, 2001; revised manuscript received February 4, 2002. Available electronically June 21, 2002.

The influence of additives on electrodeposition has been investigated for many years, and many experience-based observations and hypotheses of mechanism have been put forward.[1-5] In addition, a variety of new experimental tools[6,7] are providing remarkable data at the molecular level, from which improved physical insight and hypotheses of mechanism are emerging. It is clearly important to develop improved engineering procedures for incorporating new molecular understanding about additives into mathematical models of electrodeposition systems.

The practice of electrodeposition and the effect of additives have been recently reviewed.[8,9] In the present work, we consider the behavior of a hypothetical additive that behaves in a manner described first by Kardos and Foulke.[10-14] That is, the additive blocks deposition but is consumed at the cathode surface, while its arrival proceeds under transport-limited conditions so that more additive arrives at the peaks than in the valleys of the surface. Leveling of an irregular surface therefore occurs because the higher concentration of blocking additive on the more accessible peaks decreases the deposition rate there in comparison with the valleys.

Simulations[15,16] of the transport processes associated with deposition have been carried out for the Kardos-Foulke mechanism. In addition, Madore *et al.*[17] used the Kardos-Foulke mechanism to describe leveling during electrodeposition into trenches and grooves, and reported good agreement with experiments for nickel electrodeposition in the presence of coumarin.[18,19] Roha and Landau[20] also developed a transport-reaction model based on the Kardos-Foulke mechanism and obtained polarization curves with features typical of additive systems.

The presence of trace amounts of multiple additive compounds is essential for many electrodeposited structures of high quality such as used for on-chip copper interconnects in microelectronic devices.[21,22,23] A variety of continuum models have recently been reported that clarify important aspects of behavior. Takahashi and Gross[24] studied transport phenomena during in-filling of submicrometer trenches and, among other observations, reported that diffusion is the major transport limitation inside the trench. West *et al.*[25] used a pseudo-one-dimensional simulation to study pulse reverse effects in the filling of trenches, and also to estimate the relative importance of various system parameters.[26] Georgiadou *et al.*[27] used finite difference and finite element methods to simulate shape evolution during in-filling of a trench by electrodeposition with an additive.

Traditional electrochemical engineering methods, however, are based on continuum equations that have a blind spot at the molecular scale where critically important events associated with additives determine product quality. In Part I of this series, a linked continuum/noncontinuum approach was used to articulate a hypothesis of molecular mechanism for copper electrodeposition in additive-free solution. In Part II, we extend the hypothesis of mechanism to include the effect of an additive species that follows the Kardos-Foulke blocking mechanism. In addition, we use the linked continuum/noncontinuum approach to simulate in-filling of small trenches, an application for which improvements are urgently needed in both scientific understanding and engineering procedures.

Hypothesis of Mechanism for Hypothetical Blocking Additive

The hypothesis of mechanism for copper electrodeposition presented in Part I is used here without change except for the addition of a blocking additive into the system. A schematic representation of the mechanism is shown in Fig. 1. Cu^{2+} ions (white circles) diffuse to the surface where they are reduced by a one-electron reaction to Cu^{+} ions (gray circles) that adsorb on the surface where they move by surface diffusion to a second site where reduction occurs by a second one-electron reaction to copper atoms (dark gray squares). To this underlying mechanism, we add the presence of a hypothetical blocking additive. The additive (species A in Fig. 1) diffuses to the surface where it adsorbs and thus blocks some of the sites from availability to the adsorption of Cu^{2+}. The additive can slowly break down to form debris (species D in Fig. 1), losing its ability to block the copper reaction. In addition, the growing Cu deposit may entrap the additive.

The molecular hypothesis of mechanism was used to carry out Monte Carlo calculations in a simulation space that consisted of a cubic lattice in which species were represented by blocks in the lattice, referred to in the following description as ''particles.'' The adsorbed additive was assigned the property that it created an impassible energy barrier for the occurrence of Cu^{2+} adsorption on any site adjacent to an adsorbed additive particle. Therefore the adsorbed additive particles adversely affected the adsorption of Cu^{2+} by reducing the number of available sites on the surface. In addition, setting the Cu^{2+} adsorption energy barrier high on neighboring sites prevented adsorption of Cu^{2+} on sites adjacent to any of the six faces of the additive particle. The adsorbed additive therefore also has an effect on surface diffusion of Cu^{+} by blocking surface sites from access to diffusing adions. An adsorbed additive particle was assigned a slow breakdown reaction rate by which it is converted to a debris particle that was removed from the simulation (to reduce computations) once it was found to be desorbed from the surface.

The ''continuum'' region far from the reactive surface was described by a one-dimensional finite difference code as described in

* Electrochemical Society Student Member.
** Electrochemical Society Fellow.
z E-mail: r-alkire@uiuc.edu

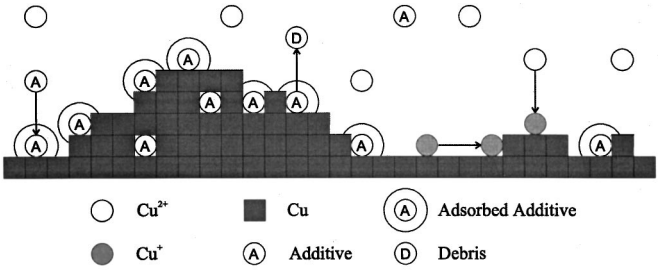

Figure 1. Schematic representation of the reaction mechanism for Cu electrodeposition in the presence of a blocking additive.

detail in Part I. The code provided a flux at the interface between it and the Monte Carlo code. In turn, the Monte Carlo code provided a concentration to the continuum code.

For the simulations carried out in this paper, values of the parameters associated with the various steps in the overall reaction mechanism are given in Table I. The parameters for the copper particles were the same as the ''base case'' that was chosen with use of experimental data as described in Part I of this series. The bulk diffusion rate of the additive particles was assumed to be the same at the Cu^{2+} ion. We did not attempt to define the ratio of the number of moles of additive in a block in comparison with the number of copper ions, and arbitrarily used the value of one. For this reason, the additive concentrations that appear in the following discussion are described in terms of ''concentration units'' rather than molar or other specific units. The remaining values for parameters associated adsorption and breakdown rates for the hypothetical additive were chosen arbitrarily so as to have a clear effect on trench filling. An overpotential of 300 mV was selected for the simulations since it was found to minimize computational requirements. That is, a higher value required smaller time steps to accommodate the more rapid reaction, while a lower value required a longer simulation time for the trench-filling to occur. In future publications, we will report experimental data for various additive systems, along with refined mechanistic information and associated parameters.

Numerical Methods

The Monte Carlo code described in Part I was modified to include additive particles. The size of the Monte Carlo space was 70 blocks wide, 120 blocks tall, and 6 blocks deep. The trench was 40 blocks wide and 80 blocks deep using a block size of 25 nm. A typical trench-filling simulation had a time step of 1.73×10^{-7} s and computed 2.3×10^{9} time steps. The code was run on an SGI Origin 2000 running IRIX at the National Center for Supercomputing Applications at the University of Illinois. A typical trench-filling simulation took 2 days to run on a single 195 MHz R10000 processor. The size of the simulation space presented here required less then 5 Mb of memory. Tecplot was used for the visualization of the simulation results. Additional details are available in the source document.[28]

Table I. Monte Carlo parameters for additive system.

Parameter	Value
Additive bulk diffusion rate	6.0×10^{8} nm^2/s
Additive adsorption rate	1.0×10^{5} nm/s
Additive breakdown reaction rate	1.0 nm/s
Cu^{2+} adsorption energy barrier from neighbor additive	-99 J
Cu^{2+} bulk diffusion rate	6.0×10^{8} nm^2/s
Cu^{2+} adsorption rate	75 nm/s
Cu^{2+} adsorption transfer coefficient	0.339
Cu^{+} surface diffusion rate	2.0×10^{8} nm^2/s
Cu^{+} step energy barrier	-1.5×10^{-20} J
Cu^{+} broken face energy barrier	-5.0×10^{-22} J
Cu^{+} new face energy barrier	5.0×10^{-22} J
Cu^{+} incorporation rate	2.0×10^{4} nm/s
Cu^{+} incorporation transfer coefficient	-0.4
Cu^{+} incorporation transfer coefficient contributions from Cu	0.2

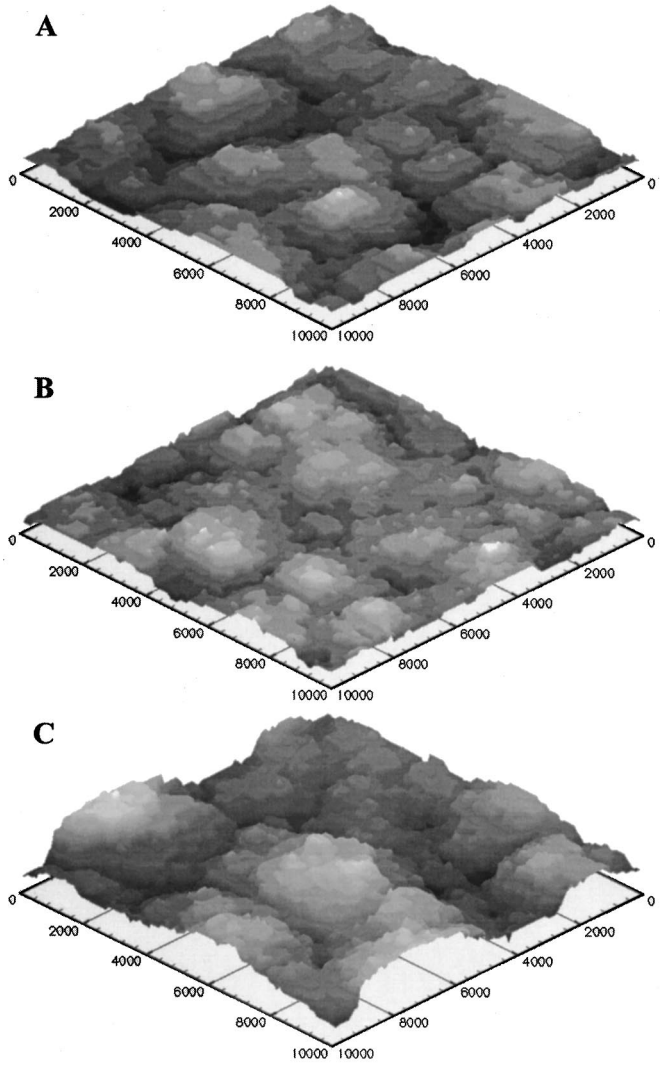

Figure 2. Simulated image of Cu deposit grown for 1000 s and calculated with parameters in Table I for blocking additive concentrations of (A) 0, (B) 0.05, and (C) 0.20 M.

Results and Discussion

The focus of the results presented here is to demonstrate the capabilities of a linked continuum/noncontinuum approach and, for a set of hypothetical additive properties, to illustrate how knowledge of molecular mechanism can be related to a prototypic technological process. It should be clear from the outset that refinements in mechanism as well as in description of the technological process are required in order to extend the approach to realistic systems.

Electrodeposition on flat surfaces.—With use of the same procedures as described in Part I, simulations were carried out to examine the influence of the additive on electrodeposition of copper on a flat surface with additive concentrations of $C_g = 0.0$, 0.05, and 0.2 concentration units. Images of the surfaces are shown in Fig. 2 for simulations with additive concentrations of $C_g = 0$, 0.05, and 0.2 units after 1000 s. The simulation with no additive (Fig. 2A) and

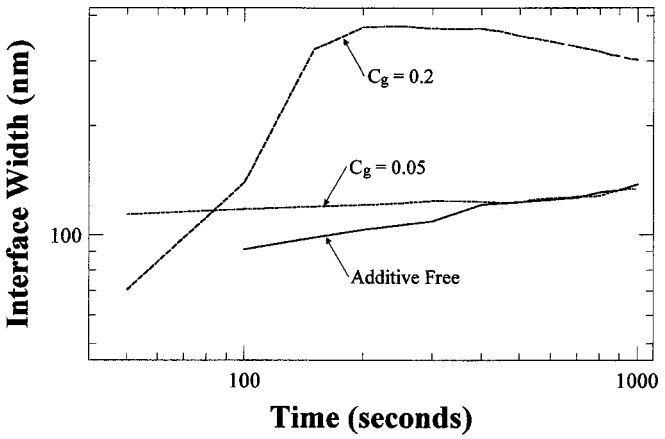

Figure 3. Scaling of the interface width obtained from numerical simulations calculated with parameters in Table I for blocking additive concentrations (C_g) of 0, 0.05, and 0.02 M.

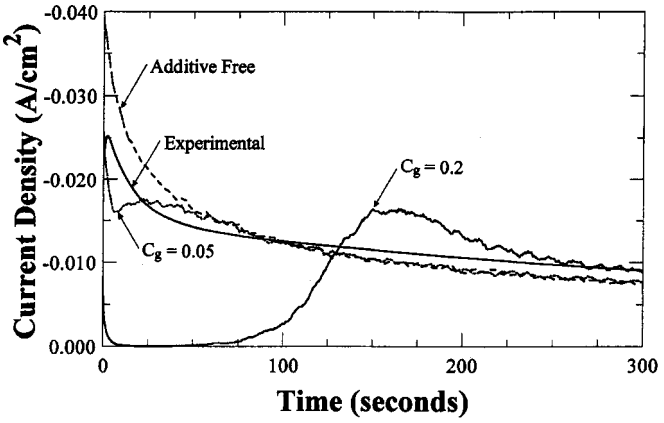

Figure 4. Comparison of experimental current-time data with numerical simulations calculated with parameters in Table I for various concentrations of blocking additive (C_g) of 0, 0.05, and 0.02 M.

0.05 concentration units (Fig. 2B) shows very similar morphologies. At high concentrations of additive (Fig. 2C) the surface produced exhibited very large bumps. In this situation it appears that parts of the surface become shut down to copper deposition, presumably due to the high concentration of adsorbed blocking additive, and the remaining locations that can support deposition produce the vertical island growth seen.

Scaling analysis of the interfacial width was applied to the simulations with additives in the same manner as in additive-free simulations reported in Part I. The scaling of the interface width with respect to time is shown in Fig. 3 for simulations with and without additive. The results for $C_g = 0.05$ concentration units are similar to the additive-free simulations above 400 s, while the additive-free simulation indicates a smoother surface time less than 400 s. By comparison, the scaling results for $C_g = 0.2$ show significantly different behavior. It can be seen that there is a fast roughening over the first 200 s, followed by gradual smoothing of the surface, presumably due to a smoothing effect produced by blocking Cu^{2+} adsorption on the tall islands causing more Cu^{2+} to adsorb in the valleys.

Simulated current-time curves for the cases with and without additive are shown in Fig. 4. The current time curve for $C_g = 0.05$ concentration units exhibits a small dip over the first 2 s but then is nearly identical to the additive-free simulation. With $C_g = 0.2$ concentration units there is a significantly different decrease in current density, presumably because a layer of additive forms rapidly on the surface before significant mass-transfer limitations set in, reducing the current to almost zero. But in time the surface coverage of additive decreases because of breakdown, and replenishment occurs at a lower level because of the diffusion limitation on its supply to the surface, resulting in a rising current. The rising current continues until mass transport of Cu^{2+} becomes a limiting factor.

Electrodeposition in rectangular trenches.—Electrodeposition in other geometries may be was simulated by replacing the bottom z-face of the Monte Carlo simulation space by the geometry of

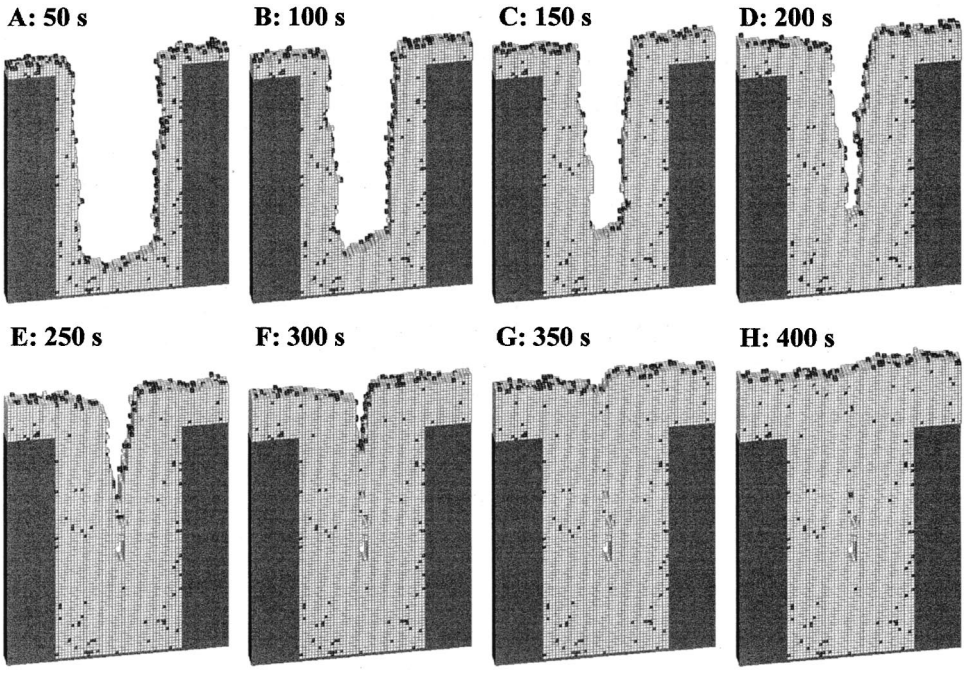

Figure 5. A sequence of numerical simulations showing eight stages during filling of a rectangular trench (sidewalls are medium gray shaded regions) by electrodeposition in the presence of a blocking additive ($C_g = 0.1$ M). Adsorbed/entrapped additive blocks are depicted in black.

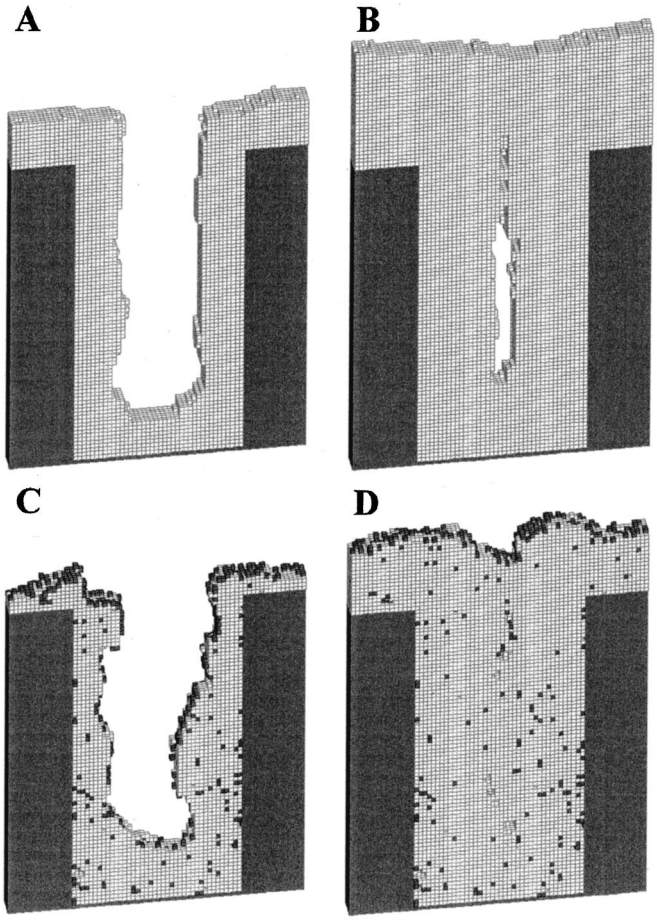

Figure 6. Numerical simulation of electrodeposition in a rectangular trench without additive for (A) 500, (B) 1000 s, and with additive (C_g = 0.225 M) for (C) 500 and (D) 1000 s.

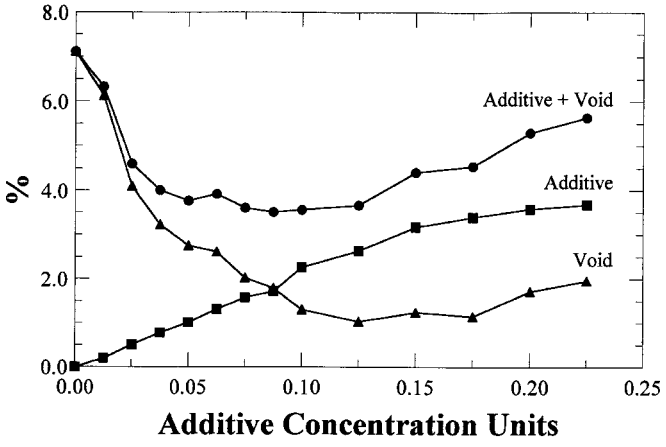

Figure 7. Predicted effect of blocking additive concentration (C_g, M) on percentage of entrapped additive and void space in trench deposit. See Table I for other system parameters.

interest. In the following paragraphs, results for a rectangular trench are described. The base case for the additive simulations used a concentration of C_g = 0.1 units. The trench width and block size were chosen to keep down computational requirements while at the same time maintaining a reasonable resolution in the trench. For these reasons, we selected a trench geometry of 1000 nm wide by 2000 nm deep as the base case. A block size of 25 nm was used, resulting in a trench that was 40 blocks wide and 80 blocks deep.

A series of ''snapshots'' taken every 50 s during trench filling is shown in Fig. 5 for the base case. It may be seen that the trench initially filled in a conformal manner in the lower portions of the trench, but slightly slower on the upper parts of the trench and exterior surface. At approximately 250 s the in-fill pinched off a small void midway down into the trench. The rest of the filling progresses on the surfaces of a deep ''V'' shape. Once the trench is finished being filled, the external surface grows evenly. Similar shape evolution results have been simulated using continuum models.[27]

The effect of additive concentration.—The concentration of additive in the deposition bath was varied between 0 and 0.225 concentration units. Images for two concentrations are shown in Fig. 6 for deposition times of 100 and 400 s. Figure 6A and B provides results in additive-free solution and it is seen that a large void appeared in the deposit. Poor in-filling without additive is a result of Cu^{2+} preferring to adsorb on the upper parts of the trench because it is geometrically more accessible to Cu^{2+} diffusing in from the bulk solution. Comparable results for 0.1 and 0.225 concentration units are seen in Fig. 5B and H, and Fig. 6C and D, respectively. From the 400 s results in Fig. 5H and 6D it can be seen that the remnant void size decreased as the concentration of additive was increased. The decrease occurs because the additive adsorbs on the upper parts of the trench, blocking Cu^{2+} adsorption, allowing the Cu^{2+} to diffuse further into the trench without being consumed. The increased concentration of additive also results in larger amounts of entrapped additive. At high concentrations, Figs. 6C and D, the additive is seen to cause the trench to fill in a more nonuniform manner, a result of blocking large patches on the surface so that the remaining active areas grow faster because they are the only growth spots.

The effect of additive concentration on the percentage of entrapped additive, void space, and the sum of additive and void space is shown in Fig. 7. The calculated values in Fig. 7 only represent the material inside of the trench and not material deposited above the lip of the trench. As was seen in the previous above images, an increase in additive concentration results in a decrease in void space, except at very high concentrations an increase in void space is seen. A steady increase in entrapped additive with increased concentration is also seen. An increase in entrapped additive with increased concentration has been reported experimentally for thiourea.[29,30]

The effect of additive adsorption rate.—To investigate the effect of additive adsorption rate on trench filling, a base case of C_b = 0.1 concentration units and an additive adsorption reaction rate of 1.0 $\times$ 10^5 nm/s were selected. Additional simulations were carried out with for adsorption reaction rates between 1.0 $\times$ 10^3 and 10^7 nm/s. Results for 100 and 400 s for different adsorption rates are shown in Fig. 8. At low adsorption rates (Fig. 8A and B) a large void space can be seen which decreases in size with increasing adsorption rates. In the 100 s images (Fig. 8A and C) it can be seen that the additive appears to adsorb evenly at low adsorption rates but primarily on the upper parts of the trench at higher adsorption rates. Based on simulations reported in the thesis,[28] it was found that the trench filling occurred in a conformal manner for adsorption rates less then 3.2 $\times$ 10^4 nm/s, but at higher adsorption rates the trench filled faster from the bottom. At an adsorption of 1.0 $\times$ 10^6 nm/s the trench filled in a ''V'' shape. Figure 8C illustrates the case found for adsorption rates higher than 1.0 $\times$ 10^6 nm/s, where the additive had trouble penetrating into the trench, causing the upper parts of the trench to fill in a ''V'' shape while the lower parts fill in a more conformal fashion. This figure also shows clearly that the amount of entrapped additive at the bottom of the trench was low for the high adsorption rates.

The effect of additive adsorption rate on the percentage of entrapped additive, void space, and the sum of additive and void space is shown in Fig. 9. As seen also in the accompanying images, with

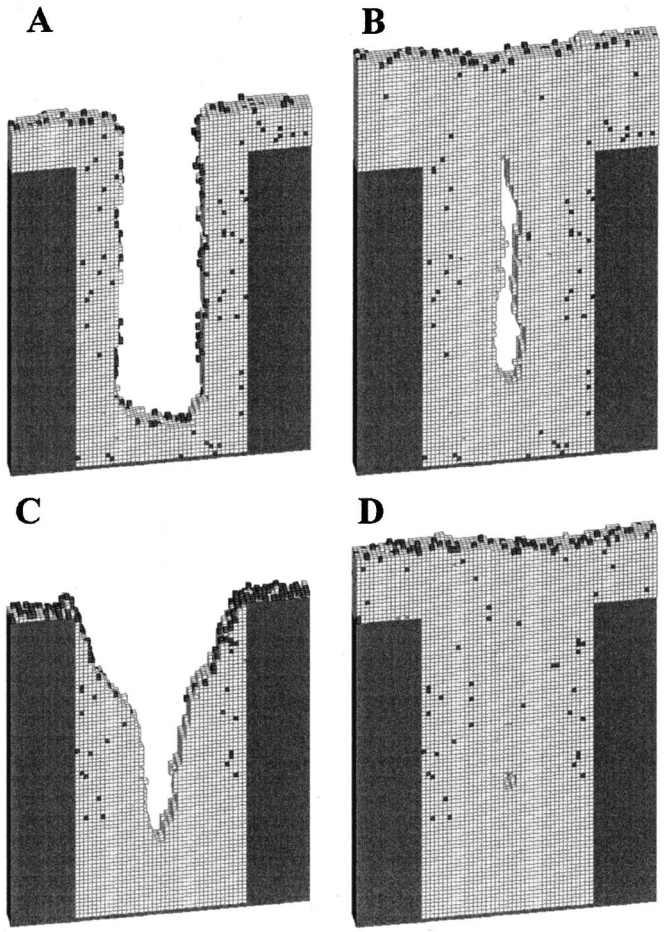

Figure 8. Effect of blocking additive adsorption rate (R_{g1}, nm/s) on evolution of shape during electrodeposition in a rectangular trench. $R_{g1} = 10^3$ nm/s for (A) 100 and (B) 400 s, and $R_{g1} = 10^7$ nm/s for (C) 100 and (D) 400 s.

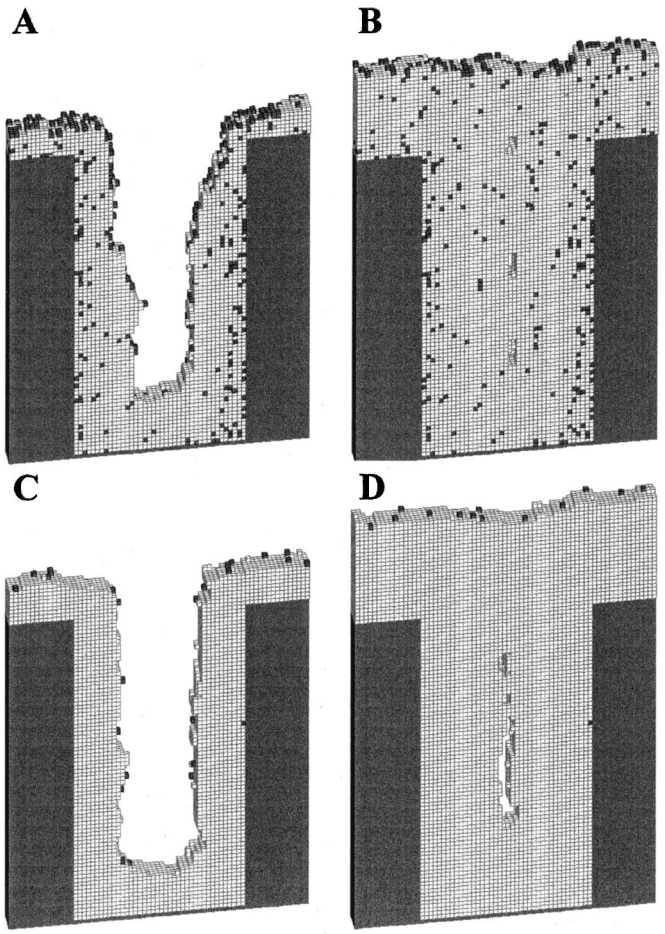

Figure 10. Effect of blocking additive desorption rate (R_{g2}, nm/s) on evolution of shape during electrodeposition in a rectangular trench. $R_{g2} = 0.56$ nm/s for (A) 100 and (B) 400 s, and $R_{g2} = 10$ nm/s for (C) 100 and (D) 400 s.

an increase in adsorption there is a decrease in void space. The amount of entrapped additive is seen initially to increase with adsorption rate and then to decrease. The increase is caused by more of the additive being able to adsorb; the decrease occurs because the additive adsorbs on the external surface and entry region of the trench, and little is left to diffuse and adsorb deep inside the trench.

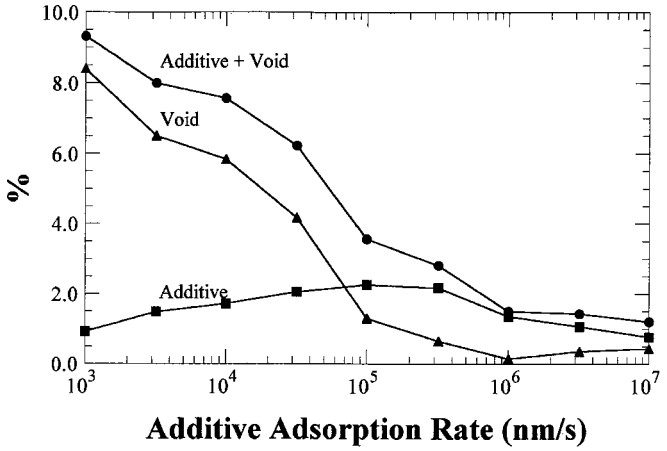

Figure 9. Predicted effect of blocking additive adsorption rate (R_{g1}, nm/s) on percentage of entrapped additive and void space in trench deposit. See Table I for other system parameters.

The effect of additive breakdown.—With use of the base case values for other parameters, the additive breakdown rate was varied between 0.56 and 10.0 nm/s to investigate its effect on filling. For low breakdown rates (Fig. 10A and B) the amount of entrapped additive is high since it has less of a chance to escape from the surface before it becomes entrapped. For high breakdown rates (Fig. 10C and D), larger void spaces were found, along with lower amounts of entrapped additive. At high desorption rates the additive gets removed from the surface quickly and its ability to affect the filling of the trench is decreased. At the high desorption rates the filling begins to look like deposition in a trench without additives (Fig. 6A and B).

The effect of the additive desorption rate on the percentage of entrapped additive, void space, and the sum of additive and void space is shown in Fig. 11. As was seen with the images in Fig. 10, an increase in desorption rate corresponded to an increase in void space. The amount of entrapped additive is seen to be very low at high desorption rates but increases very quickly at lower desorption rates.

The effect of aspect ratio.—The aspect ratio (height to width) of the trench was also modified to see the effects on the filling of the trench while holding other variables at their base values. Results are shown in Fig. 12 for aspect ratios of 0.5, 1, 3, 4, and 6; the case for an aspect ratio of 2 is shown in Fig. 5H. It may be seen that the trenches filled with relatively little formation of a central void up to

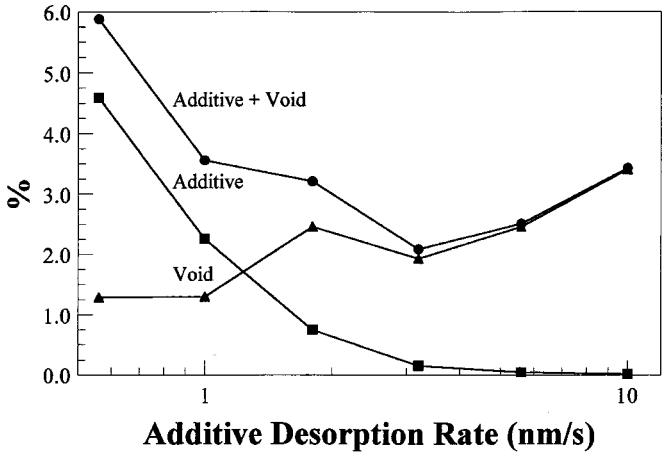

Figure 11. Predicted effects of blocking additive desorption rate (R_{g2}, nm/s) on percentage of entrapped additive and void space in trench deposit. See Table I for other system parameters.

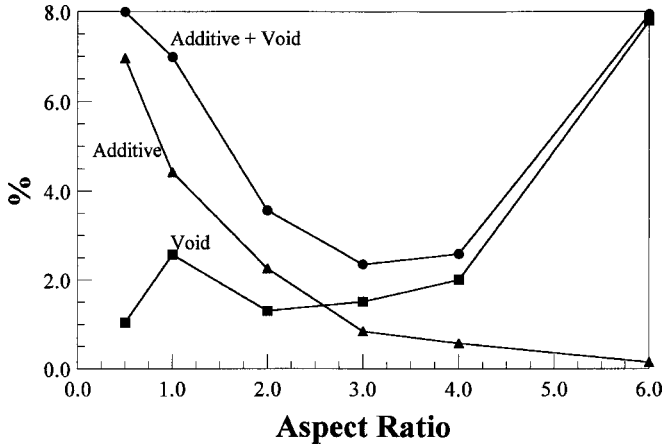

Figure 13. Predicted effect of trench aspect ratio on percentage of entrapped additive and void space in trench deposit. See Table I for other system parameters.

an aspect ratio of 4 (Fig. 12E), except for a small seam line where little voids form along the center line of the trench. At an aspect ratio of 6 (Fig. 12F) a large void forms at the bottom of the trench. The void size at an aspect ratio of 6 is due in part that the trench is so deep that very little Cu^{2+} diffuses to the bottom of the trench. It can also be recognized that as the aspect ratio increased the amount of entrapped additive decreased. We explain this by noting that an increased surface area and thus a lower growth rate per area accompanied an increase in aspect ratio, since the overall process is diffusion limited. The slower growth rate allows the additive more time to break down and thus not become entrapped. The formation of voids in high-aspect-ratio geometries has also been simulated with continuum models.[27]

The effect of the aspect ratio on the percentage of entrapped additive, void space, and the sum of additive and void space is shown in Fig. 13. As seen with these images, with an increase in aspect ratio there is a decrease in entrapped additive and increase in void space.

Conclusions

A hypothetical blocking additive was introduced into the simple Cu deposition model. On a flat surface at low concentrations numerical results indicated that the additive produced rougher surfaces at short times than the additive-free system but did not roughen as fast as the additive-free system. At high concentrations the simulations indicated that the additive caused the surfaces to roughen markedly while other sections of the surface did not. Such results can be tested by comparisons to experimental data.

The blocking additive system was used in numerical simulations of trench in-filling. Without an additive, simulations indicated that a void was to be expected in the deposits due to preferential deposition on the portion of the trench closest to the bulk solution where diffusion is most rapid. The addition of a blocking additive was found to decrease the size of the void space because it limits adsorption of Cu^{2+} on the upper parts of the trench and thus causes increased rates of deposition inside the trench. The additive was also found to become entrapped inside the Cu deposit.

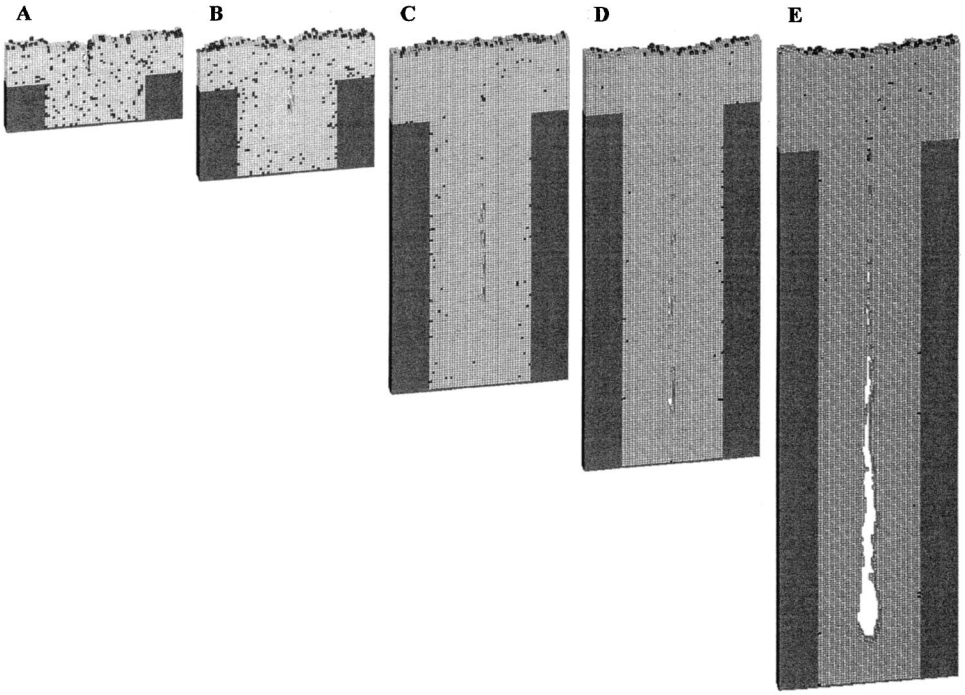

Figure 12. Effect of trench aspect ratio on evolution of shape during electrodeposition in a rectangular trench. Aspect ratio is (A) 0.5, (B) 1, (C) 3, (D) 4, and (E) 6. See Table I for other system parameters.

Simulations also demonstrated that the concentration of blocking additive has an effect on the in-filling of a trench. At low concentrations there was little effect on filling. As the concentration was increased, the void space was found to decrease. At high concentrations the void space was seen to increase again. The amount of entrapped additive was also seen to increase with increased concentration.

The adsorption rate of the additive was found to have an important role in trench filling. Low adsorption rates were similar to not having any additive, resulting in a large void. With an increase in adsorption rate the void space was found to increase. At high adsorption rates the trench filled predominantly from the bottom, forming a ''V'' shape while filling.

The rate of additive breakdown had a similar effect as the concentration of additive. With higher reaction rates the void space increased and the amount of entrapped additive decreased. Higher reaction rates had the effect of lower concentration by lowering the effectiveness of the additive.

The aspect ratio of the trench was shown to have an effect on the filling of a trench. With increasing aspect ratios the amount of void space was seen to increase. The amount of entrapped additive was seen to decrease with increased aspect ratios, a result of slower deposition per area caused from the increase surface area of the trench at higher aspect ratios.

The hypothetical additive, although simple in many respects, captures some of the effects seen in real systems. Clearly the trends predicted by the model can be tested by an experimental program. The hypothetical additive provides a starting point to compare to real additives and for deriving more realistic mechanisms. The Monte Carlo model that has been developed is flexible and expandable to allow for much more complex model additives and multiadditive systems to be developed.

Acknowledgments

This material is based upon work supported by the U.S. Department of Energy, Division of Materials Science, under award no. DEFG0296ER45439, through the Frederick Seitz Materials Research Laboratory at the University of Illinois at Urbana-Champaign. This work was partially supported by National Computational Science Alliance under CTS970031N and utilized the NCSA SGI/CRAY Origin 2000. The work of M.J. Kushnes was supported by the National Science Foundation (CTS99-74962).

The University of Illinois assisted in meeting the publication costs of this article.

References

1. H. Fischer, *Electrodepos. Surface Treatment*, **I**, 239, 319 (1972/73).
2. T. C. Franklin, *Surf. Coat. Technol.*, **30**, 415 (1987).
3. L. Oniciu and L. Muresan, *J. Appl. Electrochem.*, **21**, 565 (1991).
4. T. C. Franklin, *Plat. Surf. Finish.*, **81**, 62 (1994).
5. E. Budevski, G. Staikov, and W. J. Lorenz, *Electrochemical Phase Formation and Growth*. VCH, Weinheim (1996).
6. *Electrolytic Metal Deposition: Fundamental Aspects and Applications*, A. S. Dakkouri and D. M. Kolb, Editors, Oldenbourg, Munich (1999).
7. *Electrochemical Nanotechnology: In-Situ Local Probe Techniques at Electrochemical Interfaces*, W. J. Lorenz and W. Plieth, Editors, Wiley-VCH, Weinheim (1998).
8. *Modern Electroplating*, 4th ed., M. Schlesinger and M. Paunovic, Editors, John Wiley & Sons, New York (2000).
9. *Fundamentals of Electrochemical Deposition*, M. Paunovic and M. Schlesinger, Editors, John Wiley & Sons, New York (1998).
10. O. Kardos and F. G. Foulke, in *Adv. Electrochem. Electrochem. Eng.*, **2**, 145 (1962).
11. O. Kardos, *Plating*, **61**, 129 (1974).
12. O. Kardos, *Plating*, **61**, 229 (1974).
13. O. Kardos, *Plating*, **61**, 316 (1974).
14. S. A. Watson and J. Edwards, *Trans. Inst. Met. Fin.*, **34**, 167 (1957).
15. J. O. Dukovic and C. W. Tobias, *J. Electrochem. Soc.*, **137**, 3748 (1990).
16. K. G. Jordan and C. W. Tobias, *J. Electrochem. Soc.*, **138**, 1251 (1991).
17. C. Madore, M. Matlosz, and D. Landolt, *J. Electrochem. Soc.*, **143**, 3927 (1996).
18. C. Madore and D. Landolt, *J. Electrochem. Soc.*, **143**, 3936 (1996).
19. C. Madore, P. Agarwal, and D. Landolt, *J. Electrochem. Soc.*, **145**, 1561 (1998).
20. D. Roha and U. Landau, *J. Electrochem. Soc.*, **137**, 824 (1990).
21. P. C. Andricacos, C. Uzoh, J. O. Dukovic, J. Horkans, and H. Deligianni, *IBM J. Res. Dev.*, **42**, 567 (1998).
22. P. C. Andricacos, *Electrochem. Soc. Interface*, **8**(1), 32 (1999).
23. D. C. Edelstein, J. Heidenreich, R. Goldblatt, W. Cote, C. Uzoh, N. Lustig, P. Roper, T. McDevitt, W. Motsiff, A. Simon, J. Dukovic, R. Wachnik, H. Rathore, R. Schulz, L. Su, S. Luce, and J. Slattery, Tech. Dig. Int. Electron Devices Meet., **1997**, 773.
24. K. M. Takahashi and M. E. Gross, *J. Electrochem. Soc.*, **146**, 4499 (1999).
25. A. C. West, C.-C. Cheng, and B. C. Baker, *J. Electrochem. Soc.*, **145**, 3070 (1998).
26. A. C. West, *J. Electrochem. Soc.*, **147**, 227 (2000).
27. M. Georgiadou, D. Veyret, R. L. Sani, and R. C. Alkire, *J. Electrochem. Soc.*, **148**, C54 (2001).
28. T. J. Pricer, Ph.D. Dissertation, University of Illinois, Urbana (2000).
29. S. M. Kochergin and L. L. Khonina, *J. Appl. Chem. USSR*, **36**, 642 (1963).
30. J. Llopis, J. M. Gamboa, and L. Arizmendi, in *Proceedings of the International Conference on Radioisotopes in Scientific Research*, Vol. 2, p. 478 (1958).